ISSN: 2230-9926

Available online at http://www.journalijdr.com

IJDR

International Journal of Development Research
Vol. 10, Issue, 09, pp. 40472-40479, September, 2020
https://doi.org/10.37118/ijdr.19906.09.2020

RESEARCH ARTICLE OPEN ACCESS

USE OF GROUND PENETRATING RADAR WITH GROUND-COUPLED ANTENNA FOR DETERMINING ASPHALT LAYER DENSITY

***Paulo Roberto Antunes Aranha**

Rua Conde De Linhares 1069, 602, Brasil

ARTICLE INFO

Article History:
Received 03rd June 2020
Received in revised form
07th July 2020
Accepted 03rd August 2020
Published online 30th September 2020

Key Words:
GPR, Asphalt Pavement, Highway.

Corresponding author:
Paulo Roberto Antunes Aranha

ABSTRACT

This paper aims to analyze Ground Penetrating RADAR (GPR) as a tool for determining the density of the asphalt layer, supported by integrated testing of GPR and geotechnical data. Conventional methods for assessing the compaction control of this layer are destructive, expensive, and time consuming. The GPR technique is a remote method that is faster than existing conventional methods and has proven to be an effective tool for obtaining information during the study of highways. This methodology correlates the asphalt layer's density through the dielectric value, measured by means of a 1.6GHz ground-coupled antenna using the reflection technique. It presented satisfactory values in spite of having few sampling points, thus showing itself to be a good alternative for indirectly determining the density of the hot mix asphalt concrete (HMAC) layer and for future work in this area.

Citation: ***Paulo Roberto Antunes Aranha. 2020.*** "Use of ground penetrating radar with ground-coupled antenna for determining asphalt layer density", *International Journal of Development Research*, 10, (09), 40472-40479.

INTRODUCTION

Ground Penetrating RADAR (GPR) is a noninvasive, continuous high speed tool for data collection that has been used to map subsurface conditions in several applications. (ANNAN A. P., 1992; KNOLL e KNIGHT, 1994; ARANHA et al., 2002; SAARENKETO, 2006; LOIZOS e PLATI, 2007; FARIA, 2010). However, this tool's history is relatively recent. The RADAR emits electromagnetic pulses into a medium. When it finds a significant contrast in the materials' electrical properties that are above and below this interface, part of the energy is reflected back while the remainder continues downward, being reflected again by another interface or totally absorbed by the medium.

The high resolution image obtained is called a radargram and constitutes the basis for interpreting and constructing the profile of the existing pavement. Image quality can vary due to the characteristics of reflected, refracted, and diffracted pulses; pulses are conditioned by the dielectrical properties of the materials investigated and their interaction with the medium in which they are inserted, as well as by the antenna frequency. These GPR systems typically have the following components: a pulse generator using a given frequency and potency, one or more antennas which transmit through the subsurface, and a sorter and data recorder which captures and stores the signals reflected by the medium. Fig. 1 shows how data is obtained using horn antennas.

Data recorded by reflection of the wave in the interfaces shown in Fig. 1 can be interpreted to infer the substrata's properties with respect to compaction. This data, typically a GPR scan, present in the reflections at the interfaces 1, 2 and 3 of Fig. 1, can be seen in Fig. 2. In Fig. 1, interface 1 is the air interface with the asphalt layer, 2 is the asphalt interface with the base, and 3 is the base interface with the sub-base. The GPR scan is the pulse captured by the receiving antenna after the emitted pulse is reflected and refracted by interfaces and goes upward straight to the receiving antenna. In Fig. 2, A1 is the total reflection amplitude at the asphalt layer, A2 is the asphalt interface with the base, t1 is the propagation time at the asphalt layer, t2 is the time taken to go through the base layer, noting that these times are the signal's penetration and reflection travel times (two-way travel times) (SAARENKETO, 2006).

The GPR's basic working principle is that, knowing the time ($\boldsymbol{t}$) and the velocity ($\boldsymbol{v}$) of pulse propagation, it is possible to determine the distance ($\boldsymbol{d}$) between the object and the pulse's emitting source (SAARENKETO, 2006).

$$d = \frac{v \times t}{2} \quad (1)$$

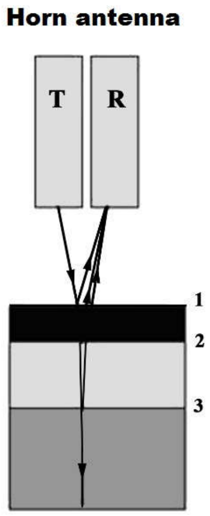

Fig. 1. Basic principle of GPR technique using horn antenna for pavement analysis, where T is the transmitting antenna and R is the receiving antenna (Adapted from SAARENKETO, 2006)

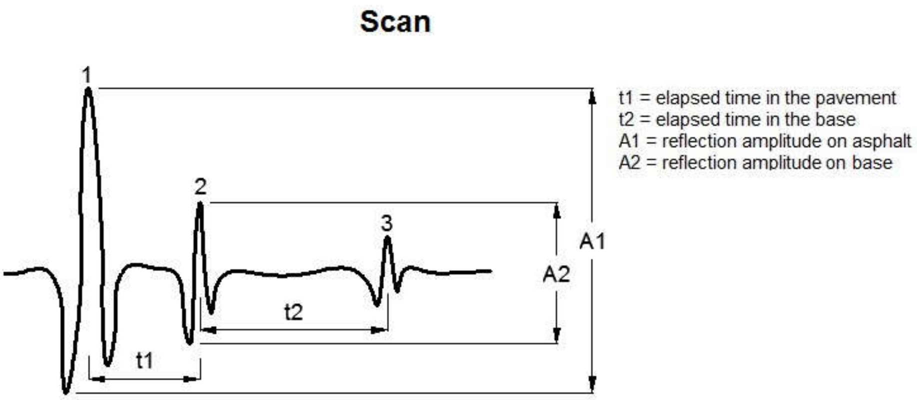

Fig. 2. Schematic of a GPR scan. (Adapted from SAARENKETO, 2006)

The asphalt layer's dielectric value can be measured with a GPR antenna using the reflection technique. This technique is based on the reflection and refraction properties of the electromagnetic waves emitted by the GPR system. A key advantage of this method is that it generates a continuous series of readings for pavement when coupled to a vehicle with speed compatible with the road's operating (SAARENKETO, 1997). The values of the specific dielectric constants of the layer are calculated from the interfaces' reflection amplitude, and these amplitudes are compared with the reflection of the electromagnet wave emitted by the GPR on a metal plate (perfect reflector), i.e., it possesses 100% of the signal reflected (SAARENKETO, 2003). With the information from the amplitudes (measured in volts in analogical systems and bits in digital systems) and measuring the time between the peaks of the reflections, it is possible to calculate the value of the dielectric constant, (Eq. 2) (SAARENKETO e SCULLION, 2000):

$$\varepsilon_a = \left(\frac{1+\frac{A_1}{A_m}}{1-\frac{A_1}{A_m}} \right)^2 \quad (2)$$

Where:

ε_a = dielectric constant of the asphalt surface layer;
A_1= amplitude of the reflection on the surface measured peak to peak;
A_m= amplitude of reflection on a metal plate.

According to Saarenketo (2006), Equation 2 works well for flexible pavements over granular bases and assumes that there is no attenuation in the surface layer emitted by the GPR, which is a reasonable hypothesis for asphalt pavements. The basic idea behind the measurements of dielectric constants is that pavement compaction reduces the void content contained in the material. Assuming that the bitumen content and the fractions of aggregates are constant, it can be said that the dielectric constant for pavement varies with changes in the void volume, i.e., the dielectric constant increases with an increase in the degree of compaction employed (SAARENKETO, 1997). This principle is illustrated in Fig. 3 below.

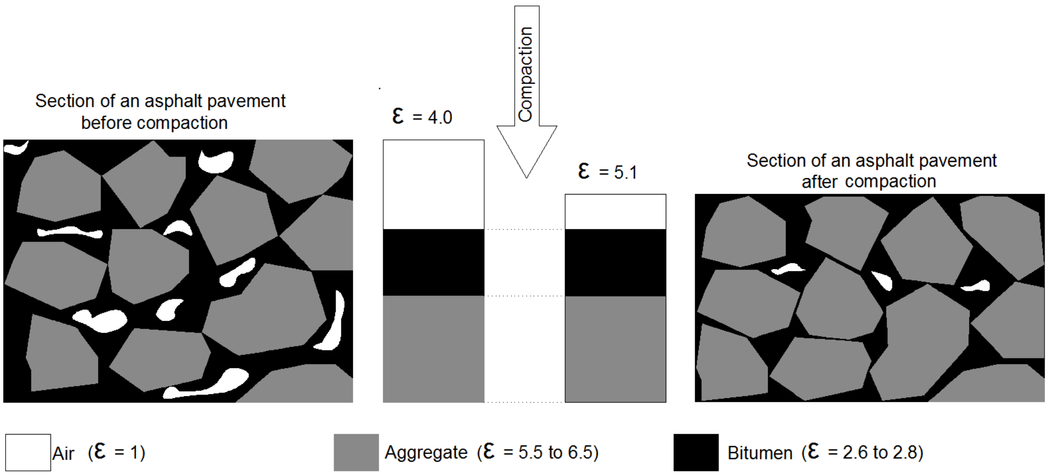

Fig. 3. Principle of the compaction effect on the asphalt dielectric constant. Adapted (SAARENKETO, 1997).

METHODOLOGY

Characterization of the study area: BR-040 is a Brazilian federal highway that is about 1148 km (713 mi) long. It starts in Brasília (Federal Capital), ends in the city of Rio de Janeiro, and goes through the Federal District, as well as the states of Goiás, Minas Gerais and Rio de Janeiro. For data acquisition, we chose a stretch of the BR 040 highway that was being widened, located at Km 470, project stake number 10381, in the municipality[1] of Sete Lagoas, MG, as shown in Fig. 4.

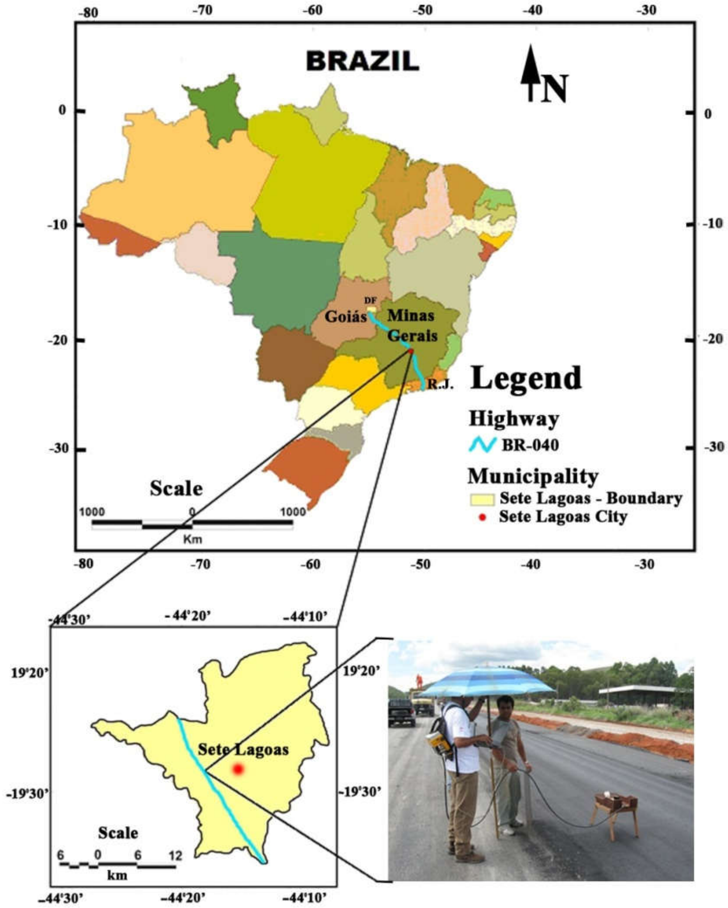

Fig. 4 - Features of the study site. BR040, Km 470, South-bound lane.

Data collection: The aim of this study is to determine the dielectric values of the asphalt layer in loose and compacted states via a "ground-coupled antenna" using the reflection technique and correlating them so that they correspond to the HMAC layer's density.

[1] *in Brazil, municipality is understood as the city and surrounding area. It is somewhat analogous to county in the United States and is distinct from the city itself.*

To use the reflection technique with a ground-coupled antenna, it was necessary to develop a bracket to suspend the antenna between 30 and 50 cm above the ground, we utilized 39 cm. In addition, we needed to use a 1m x 1m x 2 mm metal plate, regarded as the perfect reflector, as shown in Fig. 5 (SAARENKETO, 2006).

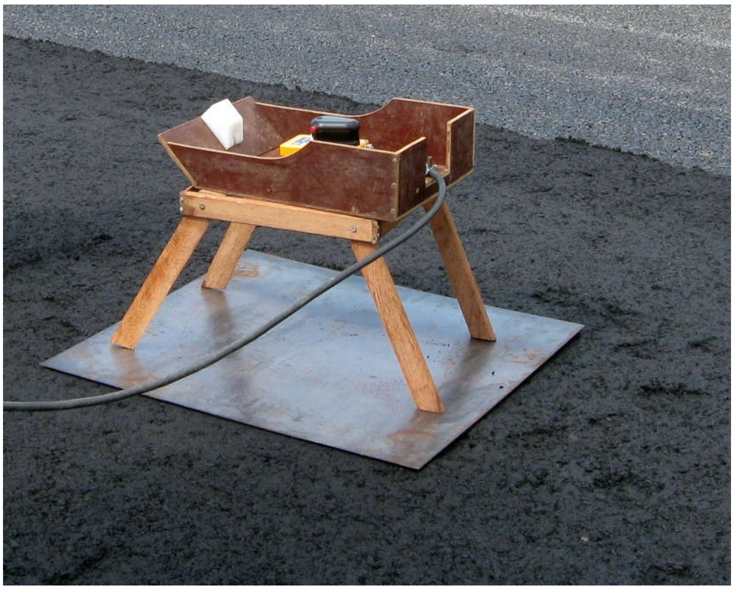

Fig. 5 - System used for data acquisition where the metal plate over loose HMAC and the wood bracket for the 1.6 GHz GPR antenna can be seen

In this test, readings were taken at two different points, one on the left edge and the other on the right edge of the lanes going from Brasília to Belo Horizonte. At each point, four readings were performed with the GPR, divided into four steps: the first step was to carry out readings on the loose HMAC without the metal plate, the second step was to carry out readings on the loose HMAC with the metal plate, in the third step readings were taken with compacted HMAC without the metal plate, and finally readings were performed with compacted HMAC with the metal plate. Fig. 06 shows the procedure described above. In each point was realized about 60 scan.

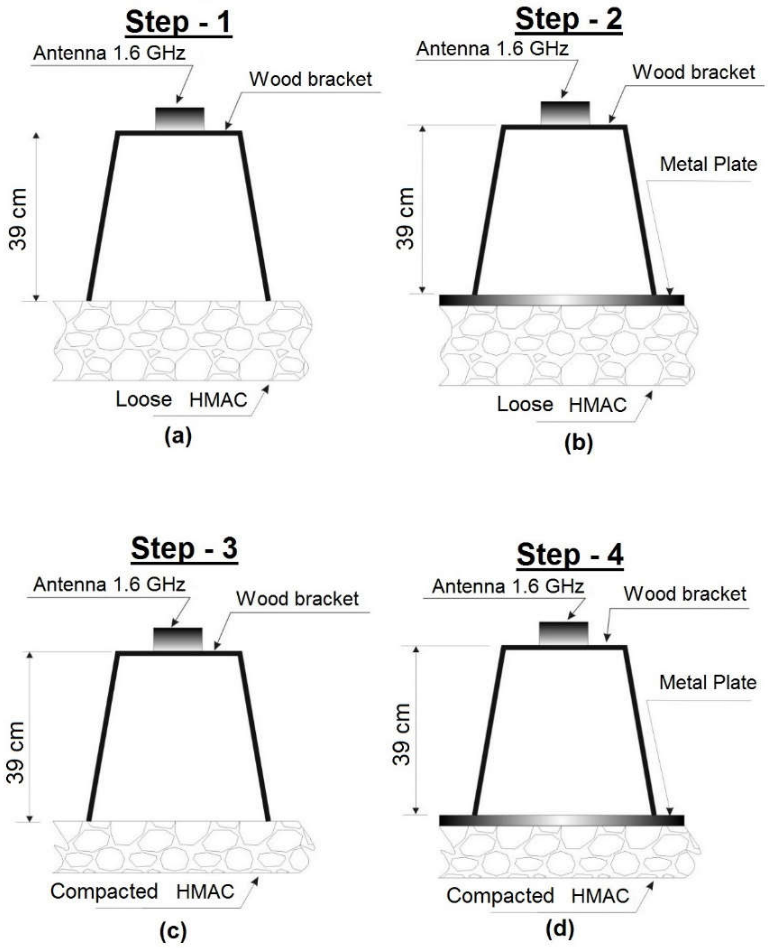

Fig. 6. Steps used to obtain results using reflection technique.

The Figs. 7 and 8 below show the radargrams obtained after steps above.

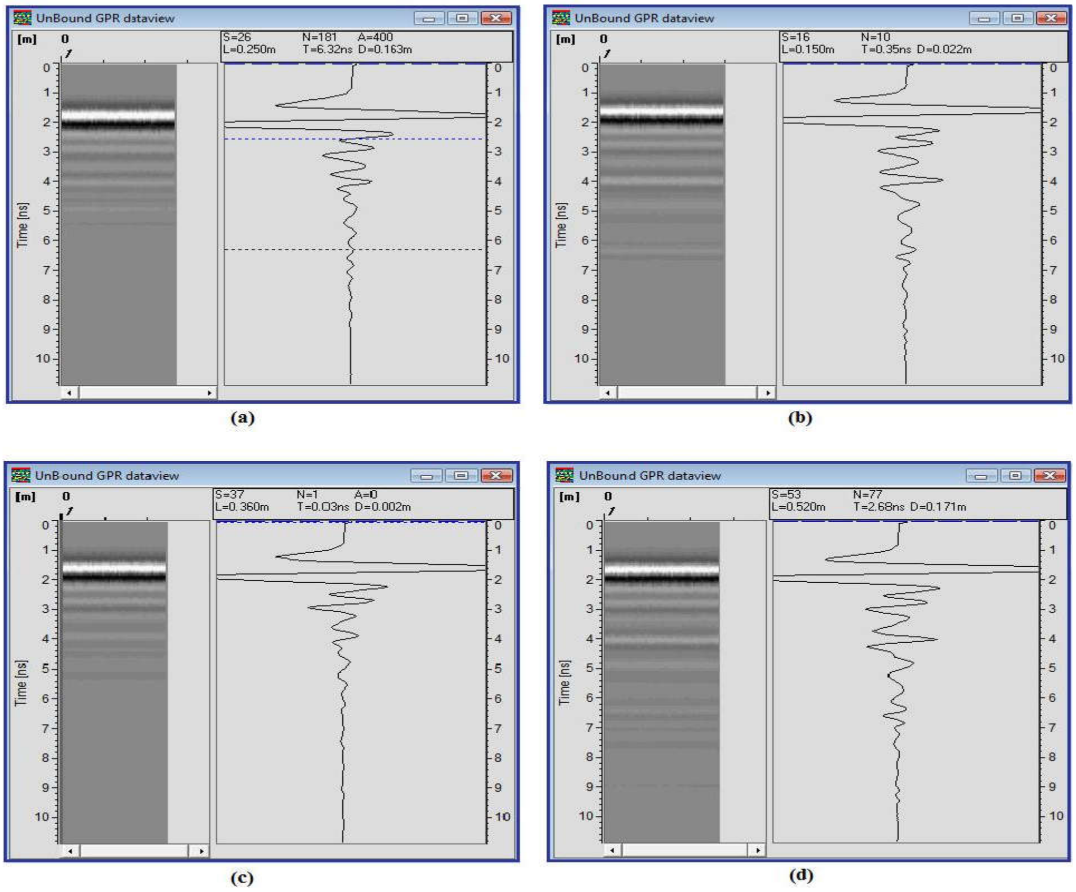

Fig. 7. “Radargrams” obtained from the left edge, lane going from Brasilia to Belo Horizonte. (a) “radargram” obtained for loose HMAC without the metal plate. (b) “radargram” obtained for loose HMAC with the metal plate. (c) “radargram” obtained for compacted HMAC without the metal plate. (d) “radargram” obtained for compacted HMAC with the metal plate.

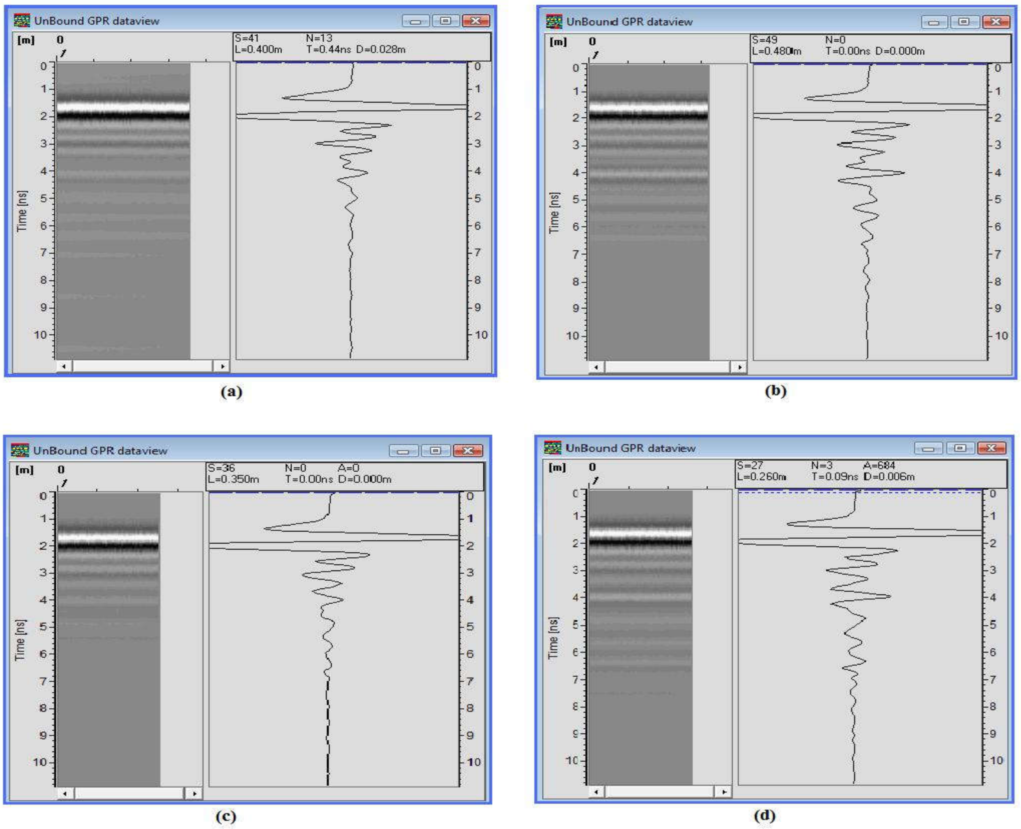

Fig. 8. “Radargrams” obtained from the right edge, lane going from Brasilia to Belo Horizonte. (a) “radargram” obtained for loose HMAC without the metal plate. (b) “radargram” obtained for loose HMAC with the metal plate. (c) “radargram” obtained for compacted HMAC without the metal plate. (d) “radargram” obtained for compacted HMAC with the metal plate

Fig. 9 below shows a radargram obtained during data acquisition with loose HMAC and with the metal plate. It also shows the amplitude reflection adopted for calculations. Remove background was not used, as it caused poorer results.

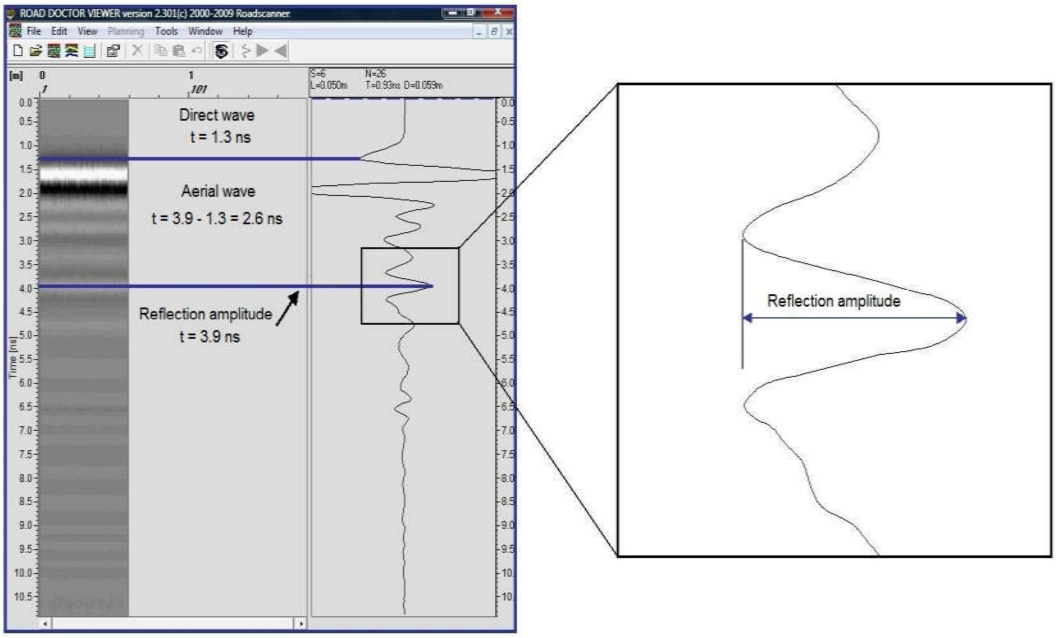

Fig. 9. Aspect of trace obtained with loose HMAC and with a metal plate.

First we removed the direct wave seen at 1.3 ns. Afterwards, to determine the position of the surface of the reflection, that is, the correct position of the amplitudes to be adopted in the calculations, we used Equation 1. That gave us the two-way travel time that the aerial wave took to run from the antenna to the ground. A numeric example is shown in Equation 3. Since the antenna was suspend 39 cm from the ground.

$$s = \frac{vt}{2} \therefore t = 2\frac{s}{v} \therefore t = 2 \times \frac{0{,}39}{0{,}3} \therefore t = 2{,}6\ ns \qquad (3)$$

After identifying the reflection amplitude at the surface at 3.9ns, via Equation 03, to be used in the calculations employing Equation 02, we used Equation 04 to return the arithmetic average of all the traces' reflection amplitude, shown in Fig. 9 (amplification), to thus have a good representative value of the reflection amplitude for each profile.

$$A_{média} = \frac{\sum_{n=1}^{tc} P_n(+)}{tc} + \left|\frac{\sum_{n=1}^{tc} P_n(-)}{tc}\right| \qquad (4)$$

Where:

$A_{média}$ = the average reflection amplitude measured from peak to peak;

tc = total of radargram columns;
$P_n(+)$ = positive peak of the n^th trace corresponding to the reflection of interest;
$P_n(-)$ = negative peak of the n^th trace corresponding to the reflection of interest

Determining the specific weight of the asphalt layer
Tables 01 and 02 show the results of calculations obtained for the highway's left and right edges, respectively. The 1st and 2nd terms of Equation 04 furnish the values presented in the columns "Peak (+)" and "Peak (-)" respectively, while the column "Average Amplitude" is given by the final result of Equation 04. The field "Dielectric Value" is obtained from Equation 02. A numeric example using Equation 02 follows:

$$\varepsilon_a = \left(\frac{1+\frac{A_1}{A_m}}{1-\frac{A_1}{A_m}}\right)^2 \therefore \quad \varepsilon_a = \left(\frac{1+\frac{5302}{7902}}{1-\frac{5302}{7902}}\right)^2 = 25{,}8 \qquad (5)$$

To validate the mathematical model, we were only able to obtain four values for the dielectric constant due to difficult field conditions. The column referring to the "Loose" state represents the material without having applied compaction energy, only having been subjected to vibration from the asphalt paver.

RESULTS AND DISCUSSION

Table 01. Dielectric values for the left edge at the study site.

Left Edge					
Stage	Peak (+)	Peak (-)	Average Amplitude	Loose / Compacted	Dielectric Value
1	3290	2012	5302	Loose HMAC	25.8
2	4030	3872	7902		
3	1351	2389	3740	Comp'd HMAC	7.6
4	3231	4668	7899		

Table 02. Dielectric values for the right edge at the study site

Right Shoulder					
Stage	**Peak (+)**	**Peak (-)**	**Average Amplitude**	**Loose / Compacted**	**Dielectric Value**
1	2582	887	3469	Loose HMA	6.7
2	4139	3692	7831		
3	2758	1146	3904	Comp'd HMAC	7.9
4	4207	3995	8202		

We observed that the value obtained for the left edge with loose (not compacted) HMAC was outside the expected range (dielectric value equal to 25.8). The dielectric value anticipated for asphalt mixtures is between 4 and 8, and, if there is slag in the mixture, this value can reach 15 (SAARENKETO, 2006). Thus, this value was discarded for validation of the equation. This error could have occurred due to interference from radios, cell phones or even from some unknown EM noise at the moment of data acquisition. The other values found, however, are coherent. A smaller dielectric value for loose HMAC was expected than for compacted HMAC due to the greater incidence of voids, which was confirmed with the exception of the point excluded (Tables 01 and 02). Further, the value obtained for compacted HMAC on the left edge was similar to that obtained on the right edge, as expected, since these two points were subjected to similar compaction energy. The results from laboratory tests for the two points sampled are summarized in Table 03 below.

Table 03. Laboratory Data for the Points Surveyed.

Elements of Analysis		***Edge***	
		Right	**Left**
Thickness (cm)	Loose	9	10
	Compacted	7.4	8.1
Specific Weight (kg/m^3)	Loose	1973	1935
	Compacted	2399	2360

Possessing data for the specific weights and the dielectric constant for the asphalt layer, a linear correlation of the data becomes possible. Fig. 10 shows the features of the line that produces correlation of the points obtained. It can be noted that, using Fig. 10 and the equation for the line that correlates the specific weight in kg/m^3 with the dielectric value of the mixture, that the expected dielectric value for loose HMAC, on the left edge where the specific weight measured in the laboratory was 1935 kg/m^3, is around 6.6 and not the value obtained with this methodology (Table 01). Figures 7 and 8 show the "radargrams" obtained on the left and right edges respectively in the lanes going from Brasília to Belo Horizonte. It is noted that there is a visible alteration in the amplitude related near the time of 4 ns, between the reading with and without the metal plate, confirming the calculations undertaken using Equation 1. The amplitudes with the metal plate show themselves to be greater than without the metal plate, demonstrating that it is a better reflector than the asphalt surface.

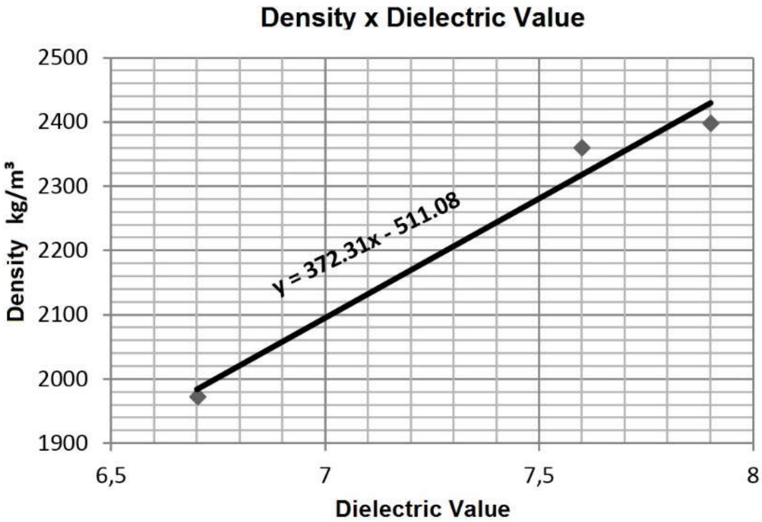

Fig. 10. Correlation of Specific Weight and Dielectric Value

Conclusions and Recommendations

The specific objectives were achieved and the methodology used for correlating the asphalt layer's dielectric constant with its specific weight using the reflection technique was shown to be satisfactory in spite of the small sample size. When comparing the results obtained in this experiment, we verify their coherence with the results obtained by SAARENKETO (2006), where the dielectric constants obtained were between 4 - 8. Nevertheless, it is worth pointing out the difficulty of finding a location to carry this experiment out with authorization from the contractor responsible for executing the service. Due to the contractor's operational difficulties, we were unable to carry out a greater number of samples, which would have further enriched this work.

Acknowledgements

We thank the Universidade Federal de Minas Gerais, Brazil, for providing the GPR system for this research and the Fundação Arthur Bernardes - FUNARBE of the Universidade Federal de Viçosa, Brazil, for the partial financial support.

BIBLIOGRAPHICAL REFERENCES

ANNAN, A. P. Ground Penetrating Radar. Workshop Notes Sensors and Annual Meeting of SAGEEP, Chicago, April 26-29. 1992.

ARANHA, P. R. A.; AUGUSTIN, C. H. R. R.; SOBREIRA, F. G., 2002. The use of GPR for characterizing underground weathered profiles in the sub-humid tropics. Jornal of Applied Geophisics, 49, 195–210.

FARIA, S. F., 2010. O uso do georadar na determinação de parâmetros da estrutura de pavimentos flexíveis. Mastership Dissertation. Universidade Federal de Viçosa, Brasil.

KNOLL, M. D.; KNIGHT, R. Relationship between dielectric and hydrogeologic properties of sand-clay mixtures. In: proceedings of the Fifth International Conference on Ground Penetration Radar, june 12-16. Kitchener, Ontario, Canada. v 1. 1994.

LOIZOS, A.; PLATI, C. Accuracy of pavement thicknesses estimation using different ground penetrating radar analysis approaches. Science Direct. NDT & E International. Vol. 40. 2007. p 147–157.

SAARENKETO, T.Electrical properties of road materials and subgrade soils and the use of ground penetrating radar in traffic infrastructure surveys. PhD thesis. Faculty of Science, Department of Geoscience, University of Oulu, P.O. Box 3000, FI-90014. Oulu: Oulu University Prees, 2006. 127 p.

SAARENKETO, T. Using ground penetrating radar and dielectric probe measurements in pavement density quality control. Paper submitted for presentation and publication at the Anual Meeting of the Transportation Research Board Washingtin, D.C. 1997.

SAARENKETO, T.; SCULLION, T. Road Evaluation with Ground Penatrating Radar. Journal of Applied Geophysics. Vol. 43. 2000. p 119 – 138.

SAARENKETO, T. Measuring electromagnetic properties of asfhalt for pavement quality control and defect mapping. 2003. Disponivel em: <http://vgwww.vegagerdin.is/nvf33.nsf/7c5e95b3edd db9e980256f620045f483/6423655ed 26a5bd400256de90031ecaf/$FILE/Asphalt_electromagnetics_TimoS_030603.pdf>. Accessed: 20 August 2008.

****